Vietnam Journal of Catalysis and Adsorption
Tạp chí xúc tác và hấp phụ Việt Nam

http://chemeng.hust.edu.vn/jca/

Study on synthesis and characterization of nano scale spinel $Mn_{0.5}Fe_{2..5}O_4$ by micro-emulsion method

Vu The Ninh[1], Dinh Xuan Loc[1], Tran Anh Tai[2]*

[1]Institute of Materials Science, Vietnam Academy of Science and Technology
[2]Van Ban High School No.3, Van Ban, Lao Cai
**Email: ninhvt@ims.vast.ac.vn*

ARTICLE INFO

Received: 16/6/2020
Accepted: 30/8/2020

Keywords:
$Mn_{0.5}Fe_{2.5}O_4$, micro-emulsion, DGDE, magnetic properties, nano scale.

ABSTRACT

The single phase of $Mn_{0.5}Fe_{2.5}O_4$ spinel crystals was prepared by the micro-emulsion method with the oil phase is DGDE (diethylene glycol diethyl ether). The characteristics of the materials have been determined by the X-ray diffraction (XRD), Energy-dispersive X-ray spectroscopy (EDX), Scanning electron microscopy (SEM) and Brunaure-Emmet-Teller (BET) nitrogen adsorption and desorption, Vibration sampling magnetometer (VSM), Fourier transform infrared spectroscopy (FTIR). The results showed that the single phase of $Fe_{0.5}Mn_{0.5}Fe_2O_4$ crystalline was formed due to the substitution of Fe by Mn in the Fe_3O_4 crystal lattice and single phase spinel crystal is formed with the size of 6.7 nm, specific surface area ≈ 193 $m^2.g^{-1}$, the saturation magnetization reaches ≈ 27 $emu.g^{-1}$.

Introduction

In the past, the application of spinel oxide materials in general and ferrite spinel oxide in particular was very wide, having multidisciplinary nature. Spinel oxide compounds have shown a huge role in engineering based on their chemical-physical properties (electrical, magnetic, optical, etc.). They are used as pigments, refractory materials, electronic engineering materials, gems, etc.[1] Nowadays, with the development of material fabrication techniques, the nano-sized spinel oxide materials are focused on research and application in biomedical and environmental fields mainly in relation to their magnetic properties.[2-4]

One of the areas where magnetic nanoparticles have the most influence is in environmental treatment, through the removal of pollutants from the groundwater and marine environments or by improving the quality of domestic water.[4] The used magnetic nanoparticles often have to meet a number of criteria such as: non-toxic, environmentally friendly, magnetic saturation is high, etc. Some ferrite spinel oxide systems with the formula AFe_2O_4 (A = Fe, Mn, Co, Zn, Cu) has been interested in research.[5] In particular, $FeFe_2O_4$ (Fe_3O_4) is not only bio-compatible, but can be made simply, so it is always the optimal choice in the research on spinel ferrit magnetic nanoparticle applications.[6]

Modified Fe_3O_4 materials always attract the attention of scientists, due to their wide applicability, as an adsorbent to remove heavy metals from polluted water sources.[5-13] The Fe_3O_4 compound can be modified by replacing Fe(II) with transition metals as shown in the formula $Fe_{1-x}A_xFe_2O_4$ (A = Mn, Cu, Co, Ni, Zn, Mg) to form the compounds have chemical stability, while improving their magnetization as well as enhancing their adsorption capacity compared to the parent compound.[11-14] Research has demonstrated, when

http://doi.org/10.51316/jca.2020.066

replacing Fe(II) with Mn(II) in the formula $Fe_{1-x}Mn_xFe_2O_4$ increases the adsorption efficiency of As, methyl orange, Congo red and some other heavy metals;[15,16] If Fe(II) is completely replaced, the removal efficiency of Cr(VI) increases in the order of $CoFe_2O_4$ < $NiFe_2O_4$ < $CuFe_2O_4$ < $ZnFe_2O_4$ < $MgFe_2O_4$ < $MnFe_2O_4$;[17] etc.

There are many proven methods to synthesize ferrite magnetic nanoparticles. Typically there are methods: co-precipitation,[6-8,13-15] micro-emulsion,[18-21] thermal decomposition,[22] hydrothermal method,[23] sol-gel,[9,24] etc. Each synthetic method has advantages and disadvantages that will be suitable for specific research and application purposes. In which, the micro-emulsion method helps to form homogeneous ferrite particles < 10 nm in size easily. In particular, the obtained material has a large surface area with a hydroxyl group (-OH) which is suitable as an adsorbent to handle water pollutants.

In this paper, presenting the survey results to determine the optimal conditions for synthesis of nanoscale $Fe_{0.5}Mn_{0.5}Fe_2O_4$ by micro-emulsion method.

Experimental

Chemicals

All reagents were analytical grade and used as received without further purifi cation. $FeCl_6H_2O$, $FeCl_2.4H_2O$, $MnCl_2.4H_2O$, NaOH, HCl and DGDE ($C_8H_8O_3$) were purchased from Sigma-Aldrich and Merck. Deionized water was used for all experiments.

Synthesis of $Mn_{0.5}Fe_{2.5}O_4$ spinel

First, prepare a solution mixture of chloride salts of the cations Fe^{2+}, Mn^{2+}, Fe^{3+}, with the following conditions: molar ratio of cation in the solution is $Fe^{2+}/Mn^{2+}/Fe^{3+}$ = 1/1/4, solution pH value = 2 - 3, the specified temperature, is called solution A. Then, while stirring an exact volume of DGDE solvent, dripping all solution A to the DGDE solvent to form the micro-emulsion phase with milky yellow color, is called solution B. Next, the co-precipitation is carried out by dripping the 1,5 M NaOH solution into solution B until the medium stabilizes with pH value = 9-10 (proceed on the mechanical stirrer). Final, Separate the precipitate, the decanter wash several times with water with external magnetic field, wash the centrifuge once with water, two times with acetone and the drying at a suitable temperature to obtain nano-ferrites.

The solvent diethylene glycol diethyl ether has boiling point 189°C, density 0.91, water solubility ≈ 100 $mg.mL^{-1}$.[25] In an acidic medium, DGDE solvent is mixed with water to form a micro-emulsion phase without the use of surfactants. On the contrary, in alkaline medium, DGDE is easy to split phase after stopping mixing with water. Therefore, the process of adjusting the pH medium not only makes the micro-emulsion process occur, but also increases the redox potential of Fe^{3+}/Fe^{2+} in an acidic medium.

In the coprecipitation reaction, there are three important factors affecting the formation of $Fe_{0.5}Mn_{0.5}Fe_2O_4$ single-phase crystals: solvent/water volume ratio (O/W), ion metal molar concentration in solution (C_M), coprecipitation process temperature (initial temperature-T_R). The co-precipitated sample was dried at 80°C for 5 hours before receiving the XRD patterns. The average crystal phase size of the ferrite spinel is determined by semi-empirical equation Scherrer (d, nm).

Characterization methods

The products obtained during different stages has been characterized by x-ray diffraction (XRD) using a D8 ADVANCE diffractometer (Bruker, Germany) with CuKα radiation (λ = 1.5046 Å) in the range of 2θ = 20° - 80°. The average crystal size of the material has been determined by the Scherrer semi-empirical equation as follows:

$$X\,(Å) = \frac{B * \lambda}{\beta * \cos\theta}$$

Where, X is the average crystal particle size, θ (degree) corresponds to angle sweeping at the maximum peak, β is width of the half maximum peak (radian), B is Scherrer constant (≈ 0.9).

Thermogravimetric and differential thermal analysis (TGA-DTA) diagrams of the samples were carried out on a Labsys EVO 1600 (Setaram, France) from room temperature to 800°C in air at a heating rate of 5°C.min^{-1}. FTIR spectra of adsorbent materials were recorded with an TENSOR II spectrometer (Bruker, Germany), using KBr pellets (KBr in a fixed ratio of 3%), in the region of 400 cm^{-1} - 4000 cm^{-1}, with a resolution of 2,8 cm^{-1}. The micro-structure image and elemental composition of sample the sample was evaluated by scanning electron microscopy combined energy dispersive X-ray spectroscopy (SEM-EDX) using a S4800 microscope (Hitachi, Japan). The specific surface area was determined by the Brunauer-Emmett-Teller (BET) method by liquid N_2 adsorption at 77K on TriStar II Plus 2.03 analyzer (Micromeritics, USA). Vibration sample magnetometer (VSM) measured on measuring equipment at Institute of Materials Science, Vietnam

Academy of Science and Technology (IMS-VAST, Vietnam).

Results and discussion

The factors affecting the formation of single phase spinel $Mn_{0.5}Fe_{2.5}O_4$ crystals

The influence of the O/W volume ratio on the formation and size of single phase of spinel ferrite crystal have shown in figure 1 and table 1. The results on the XRD patterns have shown that, the sample with O/W ratio = 4/1 is amorphous, the other samples have diffraction lines characteristic for single phase of spinel ferrite crystal. On the other hand, the results in Table 1 have shown that, when increasing the O/W ratio, the average crystal size will decrease and reach the smallest at O/W = 1/3 (9 nm). This result can be explained because increasing the O/W ratio will reduce the size and density of micro-emulsion particle, so the spontaneous heat of the coprecipitation reaction is reduced. Therefore, at the O/W ratio = 3/1, the heat radiates just enough for the crystallization of spinel ferrite, so it does not lead to the merging of small particles into larger particles. When the excess solvent (O/W > 3/1), Micro-emulsion particle concentration is too low, the heat is not enough to crystallize spinel ferrite, the precipitate is amorphous.[19]

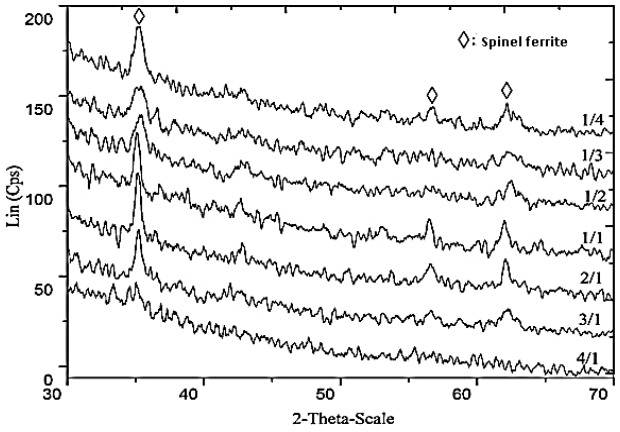

Figure 1: XRD patterns of co-precipitated samples at different O/W volume ratios

The influence of the concentration of Fe^{2+}+Mn^{2+}+Fe^{3+} in the solution phase on the formation and size of single phase of spinel ferrite crystal have shown in figure 2 and table 1. The results on XRD patterns have shown that, when reducing the cation concentration (0.25 M ≤ C_M ≤ 2 M), the average crystal size of ferrite spinel will be reduced, reaching the smallest at C_M = 0.25 (7 nm). When the metal cation concentration is too small (C_M < 0.25 M), the precipitate is amorphous (C_M = 0.1 M). This result is because when at high concentrations, the radiant heat not only provides heat to crystallize spinel ferrite, but also causes the particles to merge into larger sizes. In contrast, if the metal cation concentration is insufficient, the single phase of spinel ferrite crystal is not formed.[20]

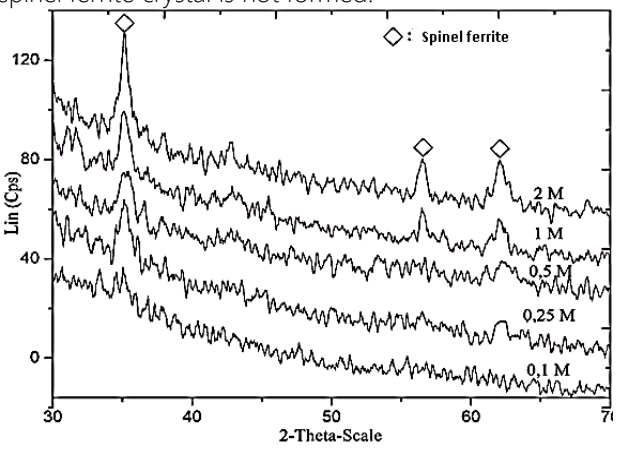

Figure 2: XRD patterns of co-precipitated samples at different metal ion concentrations

The effect of the coprecipitation process temperature on the formation and size of single phase ferrite spinel crystals have shown in Figure 3 and Table 1. The results on the XRD patterns showed that all samples formed single phase of spinel ferrite crystal with the average crystal size between samples was not different (≈ 7 nm). Thus, the temperature that initiates the coprecipitation reaction mainly plays the role of dispersing, forming and stabilizing micro-emulsion particles and the heat emitted from the coprecipitation reaction plays a major role in forming the single phase of spinel ferrit crystals.

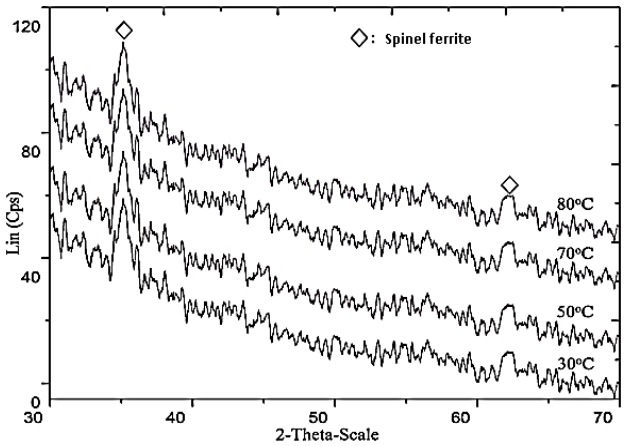

Figure 3: XRD patterns of co-precipitated samples at different temperatures

Table 1: Average crystal phase size of ferrite spinel samples was fabricated under several co-precipitation reaction conditions

http://doi.org/10.51316/jca.2020.066

Samples	O/W	C_M, mol.L^{-1}	T_R, °C	d, nm
F_1	4/1	0.50	80	-
F_2	3/1	0.50	80	9
F_3	2/1	0.50	80	10
F_4	1/1	0.50	80	13
F_5	1/2	0.50	80	19
F_6	1/3	0.50	80	21
F_7	1/4	0.50	80	23
F_8	1/3	2.00	80	16
F_9	1/3	1.00	80	12
F_{10}	1/3	0.25	80	7
F_{11}	1/3	0.10	80	-
F_{12}	1/3	0.50	80	7.1
F_{13}	1/3	0.25	35	6.7
F_{14}	1/3	0.25	50	6.8
F_{15}	1/3	0.25	65	7.0

However, the results on the XRD patterns (figure 1 - figure 3) have determined that the single phase of ferrite spinel crystal is formed, but could not demonstrate the presence and content of Mn in the sample. Therefore, the EDX spectrum analyzing F_{13} coprecipitation samples (coprecipitation conditions in Table 1) have shown in Figure 4. EDX results show that not only there are spectral peaks characteristic for the presence of Fe and O, but also characteristic peaks for the presence of Mn in the sample. From the result, the content of Fe, Mn, O atom will correspond to the formula $Mn_{0.5}Fe_{2.5}O_4$.

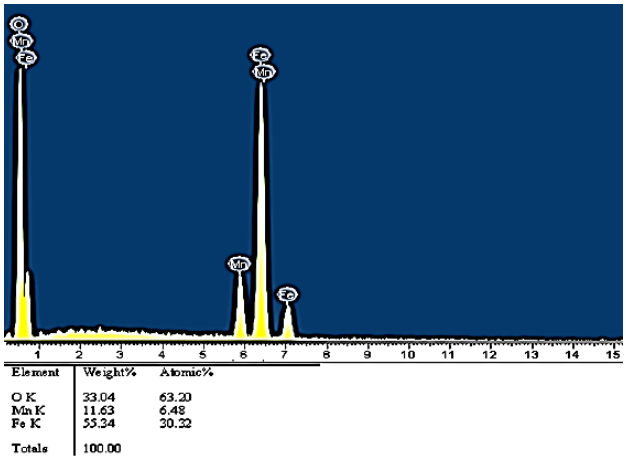

Figure 4: EDX spectra of F_{13} co-precipitated sample

Effect of heat treatment on spinel $Mn_{0.5}Fe_{2.5}O_4$

FTIR spectra analyzing the bonding group in the material when the F_{13} co-precipitated sample is dried at different temperatures have shown in Figure 5. The results on FT-IR spectra showed that the sample was dried at 80°C, with the peaks of 3446 cm^{-1} and 1629 cm^{-1} characteristic for O-H bond of free water, peak spectrum of 570 cm^{-1} characteristic for bonding M-O- (M = Fe, Mn). The sample was dried at 105°C, the spectral peaks 3419 cm^{-1}, 1625 cm^{-1} characteristic for water of crystallization, the spectral peaks 2922 cm^{-1}, 1545 cm^{-1} had low intensity characterizing the C-H bond from precursors, the spectral peaks 444 cm^{-1}, 572 cm^{-1} characterize the M-O- bond. The sample was dried at 160°C, outside of the peak spectrum of 3423 cm^{-1}, a new spectral peak 632 cm^{-1} with spectral peaks 452 cm^{-1}, 576 cm^{-1}. When the sample was dried at 200°C, with a new peak of 3405 cm^{-1} assigned to the surface -O-H bond, the three spectral peaks 454 cm^{-1}, 573 cm^{-1}, 638 cm^{-1} became sharp with high intensity. They are respectively assigned to the M(II)-O, Fe(III)-O-H and Fe (III)-O bonds. Finally, the sample heated at 300°C has a spectral peak of 3445 cm^{-1} characteristic for the O-H bond of the absorbed water, the spectral peaks 460 cm^{-1}, 575 cm^{-1} characterize the M(II)-O, Fe(III)-O bonds. This results for the fit with the DTA-TGA diagram of the sample.[6]

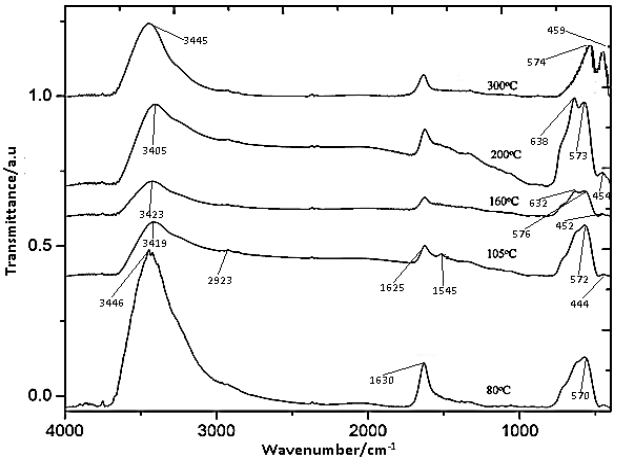

Figure 5: FTIR spectra of F_{13} co-precipitated sample were dried at different temperatures

The DTA-TGA diagram of the F_{13} co-precipitate sample have shown in Figure 6. The results on the DTA-TGA diagram showed that there are 3 effects: The first effect, endothermal and maximum at ≈ 82°C respectively reduce ≈ 6 % mass at temperatures < 200°C. This is the loss of free water and crystalline water of the sample; The second effect, endothermal and maximizes at ≈ 420°C respectively reduces ≈ 1 % mass fraction at 360°C - 600°C, respectively. This is the decomposition of the surface hydroxyl group of the sample; The third effect, exothermal and maximum at ≈ 620°C, respectively increases 0.4 % mass at 600°C - 750°C. This is the oxidation of the oxide compounds Fe(II), Mn(II) to Fe(III), Mn(III) oxide compounds. Thus, the presence of free water, crystalline water and hydroxyl functional groups on the material is one of

the important features of the co-precipitation and micro-emulsion method to make spinel $Fe_{0.5}Mn_{2.5}O_4$.[3]

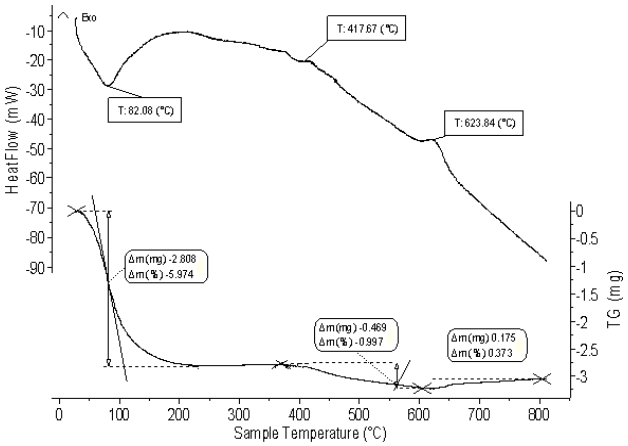

Figure 6: DTA-TGA diagram of F_{13} co-precipitated sample

XRD diagram of F13 co-precipitated samples when heated at different temperatures have shown in Figure 7. The results on the XRD patterns show that the phase spinel $Mn_{0.5}Fe_{2.5}O_4$ crystal is thermally stable to 300°C, the sample is oxidized to Fe_2O_3 phase when heated at the temperature ≥ 400°C, completely oxidation of spinel $Mn_{0.5}Fe_{2.5}O_4$ to Fe_2O_3 phase when the sample is heated at 500°C.

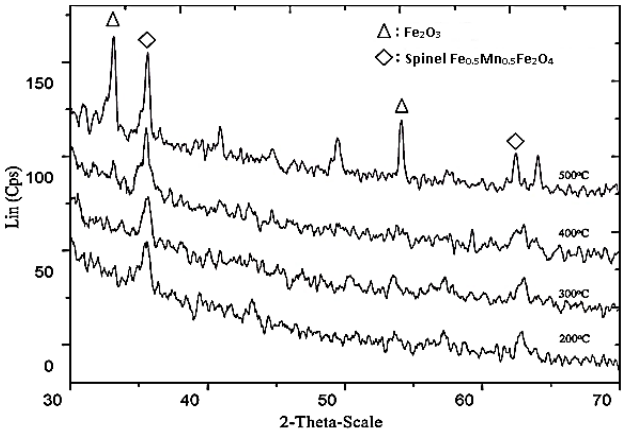

Figure 7: XRD patterns of F_{13} co-precipitated sample calcined at different temperatures

The sample has a stable phase composition of Fe_2O_3 when heated to 800°C. It can be seen that the partial or complete oxidation of spinel $Mn_{0.5}Fe_{2.5}O_4$ produces only Fe_2O_3 phase, but the absence of Mn-containing compounds. The absence of Mn-containing compounds can be explained because the spinel $Mn_{0.5}Fe_{2.5}O_4$ is oxidized to form a completely replacement solid solution with the formula $Fe_{1.66}Mn_{0.33}O_3$ and on the XRD patterns showing host phase crystal of Fe_2O_3.[26] On the other hand, when processing samples ≤ 300°C, the average crystal phase size of spinel $Mn_{0.5}Fe_{2.5}O_4$ did not change (≈ 7 nm), when heated > 300°C, the average crystal size of sample increased (400°C, 500°C respectively 18 nm, 23 nm). This XRD patterns result is quite consistent with the DTA-TGA diagram of the sample.

Characteristics of spinel $Mn_{0.5}Fe_{2.5}O_4$

The results and discussions presented in sections 1 and 2 show that spinel $Mn_{0.5}Fe_{2.5}O_4$ is formed from the coprecipitation process in the micro-emulsion phase, so the precursor is H_2O, the solvent is always exists in the form in different types of bonds. The process of heat treatment of spinel $Mn_{0.5}Fe_{2.5}O_4$ co-precipitated samples at 160°C - 400°C, the precursors were controlled and removed in stages.

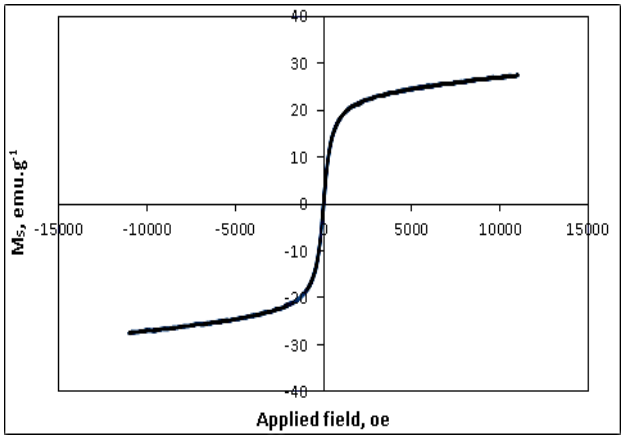

Figure 8: Magnetization curve measured at room temperature for spinel $Mn_{0.5}Fe_{2.5}O_4$ sample

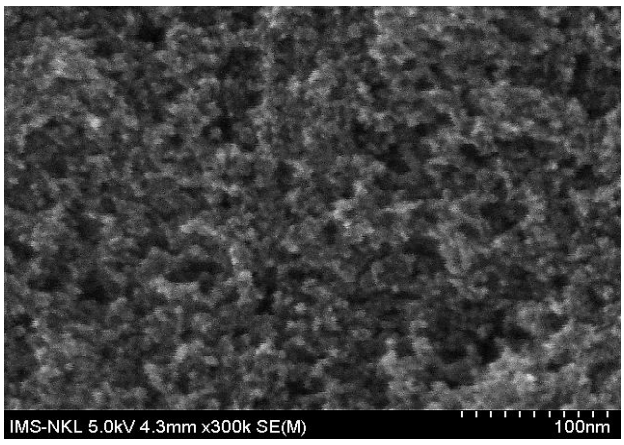

Figure 9: SEM image of spinel $Mn_{0.5}Fe_{2.5}O_4$ sample

On the other hand, in aqueous environment, heavy metal adsorption will be more efficient if the spinel $Mn_{0.5}Fe_{2.5}O_4$ magnetic nanoparticles are prepared with surface hydroxyl functional groups available. Therefore, the F_{13} co-precipitate sample dried at 200°C is the optimal spinel $Mn_{0.5}Fe_{2.5}O_4$ sample for determining several material properties such as size, specific surface

http://doi.org/10.51316/jca.2020.066

area and saturation magnetization; as well as heavy metal adsorbent material for further research.

Table 2: Parameters of some characteristics of spinel $Mn_{0.5}Fe_{2.5}O_4$ sample

Characteristic	Parameters
BET	S_{BET}: 193 $m^2.g^{-1}$
	V_{pore}: 0.24 $cm^3.g^{-1}$
	d_{pore}: 4.9 nm
Crystal	Formular: $Mn_{0.5}Fe_{2.5}O_4$
	Phase: manganese iron oxide
	d: 6.7 nm
Magnetic	Saturation magnetization: 27 $emu.g^{-1}$
	Superparamagnetic state: yes
Function	-OH: yes
SEM	Particles: yes
	d < 10 nm

In terms of surface area, table 2 shows the characteristic parameters that determine the specific surface area of the sample such as specific surface area ≈ 193 $m^2.g^{-1}$, pore volume ≈ 0.24 cm^3.g-1, size Pore ≈ 4.9 nm. Average crystal phase size ≈ 6.7 nm.

Conclusion

The single phase crystals of $Mn_{0.5}Fe_{2.5}O_4$ spinel ferrit oxide was prepared by the micro-emulsion method with the oil phase is DGDE. The optimal conditions for the synthesis of nano-sized $Mn_{0.5}Fe_{2.5}O_4$ include: O/W volume ratio = 1/3, molar concentration of total metal cation Fe^{2+}+Mn^{2+}+Fe^{3+} = 0.25 M, the coprecipitation process temperature = 35°C; The co-precipitation sample of spinel $Mn_{0.5}Fe_{2.5}O_4$ should be dried at 200°C.

Nano scale of $Mn_{0.5}Fe_{2.5}O_4$ spinel oxide was formed due to the substitution of Fe by Mn in the Fe_3O_4 crystal lattice. The single phase crystal spinel particles is is fabricated under optimal conditions has the characteristics such as the size of 6.7 nm, specific surface area S_{BET} ≈ 193 $m^2.g^{-1}$, the saturation magnetization reaches 27 $emu.g^{-1}$.

Acknowledgments

This research is funded by by Vietnam Academy of Science and Technology under grant number VAST03.06/18-19.

References

1. Phan Van Tuong, Inorganic Materials, Hanoi national university publisher, Vietnam, 1998.
2. Merzhanov A. G., Theory and Practice of SHS: Worldwide state of the art and Newest Results, International Journal of Self Propagating High Temperature, 2(2), (1993) 113-158. https://doi.org/10.3103/S1061386213040110
3. Jiang Q.L., Zheng S.W., Hong R.Y., et al., Folic acid-conjugated Fe_3O_4 magnetic nanoparticles for hyperthermia and MRI in vitro and in vivo, Applied Surface Science, 307, (2014) 224-233. https://doi.org/10.1016/j.apsusc.2014.04.018
4. Sumuel C.N.T., Irene M.C.L., Magnetic nanoparticles: essential factors for sustainable environmental applications, Water Research, 47(8), (2013) 2613-2632. https://doi.org/10.1016/j.watres.2013.02.039
5. Jozef S., Martin S., Anna G., et al., Magnetic properties of selected substituted spinel ferrites, Journal of Magnetism and magnetic Materials, 326, (2013) 251-256. https://doi.org/10.1016/j.jmmm.2012.07.016
6. Akin I., Arslan G., Tor A., et al., Arsenic(V) removal from underground water by magnetic nanoparticles synthesized from waste red mud, Journal of Hazardous Materials, 235-236, (2012) 62-68. https://doi.org/10.1016/j.jhazmat.2012.06.024
7. Trung V.Q., Trang N.T.H., Thi T.M., et al., Synthesis and Properties of Fe_3O_4/Polyaniline Nanomaterial and Its Ability of Removing Arsenic in Wastewater, Materials Transactions, 59(7), (2018) 1095-1100. https://doi.org/10.2320/matertrans.md201703
8. Babu C.M., Palanisamy B., Sundaravel B., et al., Magnetic Fe_3O_4/SiO_2 Core-Shell Nanorods for the Removal of Arsenic, Journal of Nanoscience and Nanotechnology, 13, (2013) 2517-2527. https://doi.org/ 10.1166/jnn.2017376
9. Shuang Z., Jun Y., Xiaoyan Q., et al., Magnetically recyclable $MnFe_2O_4$/polyaniline composite with enhanced visible light photo catalytic activity for rhodamine B degradation, Journal of the Ceramic Society of Japan, 124(10), (2016) 1152-1156. https://doi.org/10.2109/jcersj2.16056
10. Cai Y., Zeng G., Guo P., et al., Effective removal of Cr(VI) through adsorption and reduction by magnetic mesoporous carbon incorporated with polyaniline, Royal Society of Chemistry Advances, 4(102), (2014) 58362-58371. https://doi.org/10.1039/C4RA08432B
11. Jae G.L., Jung H.K., Kwang P.C., Crystallographic and Magnetic Properties of Zn-Mn Ferrite, Journal of the Korean Physical Society, 49(2), (2006) 604-607.
12. Tripathy D., Adeyeye A.O., Boothroyd C.B., Shannigrahi S., Microstructure and magnetotransport properties of Cu doped Fe_3O_4 films, Journal of Appied Physics, 103, (2008) 07F701-07F703. https://doi.org/ 10.1063/1.2828504

13. Giri J., Pradhan P., Somani V., et al., Synthesis and characterizations of water-based ferrofluids of substituted ferrites [$Fe_{1-x}B_xFe_2O_4$, B = Mn, Co (x = 0-1)] for biomedical applications, Journal of Magnetism and Magnetic Materials, 320, (2008) 724-730. https://doi.org/10.1016/j.jmmm.2007.08.010
14. Zhang S., Niu H., Cai Y., et al., Arsenite and arsenate adsorption on co-precipitated bimetal oxide magnetic nanomaterials: $MnFe_2O_4$ and $CoFe_2O_4$, Chemical Engineering Journal, 158, (2010) 599-607. https://doi.org/10.1016/j.cej.2010.02.013
15. Huong P.T.L., Tu N., Lan H., et al., Functional manganese ferrite/graphene oxide nanocomposites: effects of graphene oxide on the adsorption mechanisms of organic MB dye and inorganic As(V) ions from aqueous solution, Royal Society of Chemistry Advances, 8, (2018) 12376-12389. https://doi.org/10.1039/c8ra00270c
16. Wang L., Li J., Wang Y., et al., Adsorption capability for Congo red on nanocrystalline MFe_2O_4 (M = Mn, Fe, Co, Ni) spinel ferrites. Chemical Engineering Journal, 181-182, (2012) 72-79. https://doi.org/10.1016/j.cej.2011.10.088
17. Hu J., Lo I.M.C., Chen G.H., Comparative study of various magnetic nanoparticles for Cr(VI) removal, Separation and Purification Technology, 56, (2007) 249-256. https://doi.org/10.1016/j.seppur.2007.02.009
18. Okoli C., Sanchez-Dominguez M., Boutonnet M., et al., Comparison and Functionalization Study of Microemulsion-Prepared Magnetic Iron Oxide Nanoparticles, Langmuir, 28(22), (2012) 8479-8485. https://doi.org/10.1021/la300599q
19. Kale S.N., Deore S.L., Emulsion Micro Emulsion and Nano Emulsion: A Review, Systematic Reviews in Pharmacy, 8(1), (2017) 39-47. https://doi.org/10.5530/srp.2017.1.8
20. Yadav V., Jadhav P., Kanase K., et al., Preparation and evaluation of microemulsion containing antihypertensive drug, International Journal of Applied Pharmaceutics, 2018, 10(5), 138-146. https://doi.org/10.22159/ijap.2018v10i5.27415
21. Loc D.X., Huyen T.T.T., Loan N.T., et al., Synthesis and adsorption ability of $Cr_2Fe_2O_4$ spinel nanomaterials for the removal of heavy metal ions and organic dyes from industrial and domestic wastewater, Vietnam Journal of Chemistry, 57(4e12), (2019) 426-430.
22. Nam P.H., Phong P.T., Mạnh D.H., Study the structure and magnetic properties of $Co_{1-x}Zn_xFe_2O_4$ (x = 0.0-0.7) nanoparticle system fabricated by thermal decomposition method, Vietnam Journal of Science and Technology, 54(1A), (2016) 25-32.
23. Nam P.H., Uyen L.L., Thuy D.M., Manh D.H., et al., Dynamic effects of dipolar interactions on the specific loss power of $Mn_{0.7}Zn_{0.3}Fe_2O_4$, Vietnam Journal of Science and Technology, 56(1A), (2018) 50-58.
24. Loan N.T.T., Dai L.M., Synthesis of nano scale $CoFe_2O_4$ by gel combustion method, Vietnam Journal of Chemistry, 48(4), (2010) 404-408.
25. Https://pubchem.ncbi.nlm.nih.gov/compound/Diethylene-glycol-diethyl-ether.
26. Ninh V.T., Nhiem D.N., Anh N.T., Dai L.M., Preparation of nano-sized La_2O_3-Fe_2O_3-Mn_2O_3 mixed oxides for As(V) adsorption from solution, Vietnam Journal of Chemistry 55(3e12), (2017) 245-249.